Applied Microbiology and Biotechnology (2025) 109:39
https://doi.org/10.1007/s00253-025-13419-z

BIOTECHNOLOGICAL PRODUCTS AND PROCESS ENGINEERING

Recombinant CD80 fusion protein combined with discoidin domain receptor 1 inhibitor for cancer treatment

Songna Wang[1,2] · Pinliang Hu[3] · Xuyao Zhang[2] · Jiajun Fan[2] · Jing Zou[3] · Weidong Hong[3] · Xuan Huang[1,2] · Danjie Pan[2] · Huaning Chen[2] · Dianwen Ju[2] · Yi Zhun Zhu[1] · Li Ye[1,2]

Received: 19 April 2024 / Revised: 14 November 2024 / Accepted: 22 January 2025

Abstract

Immune checkpoint inhibitors (ICIs) have significantly advanced the field of cancer immunotherapy. However, clinical data has shown that many patients have a low response rate or even resistance to immune checkpoint inhibitor alone. The underlying reasons for its poor efficacy include the deficiency of immune infiltration and effective CD28/CD80 costimulatory signal in tumor. Discoidin domain receptor 1 (DDR1) has been reported to be negatively related to immune cell infiltration in tumors. Herein, we constructed a soluble fusion protein using CD80, the natural ligand of CD28, in combination with DDR1 inhibitor. Our results demonstrated that CD80-Fc effectively activated T cells and inhibited tumor growth in vivo, even in tumors with poor efficacy of ICIs. Importantly, CD80-Fc fusion protein had a milder affinity against the targets which suggested a potential higher safety than CD28 agonists. Further, in order to promote tumor immune infiltration, we attempted to combine CD80-Fc fusion protein with DDR1 inhibitor for treatment. Our results indicated that using CD80-Fc fusion protein along with DDR1 inhibitor significantly promoted T cell infiltration in tumor microenvironment and more strongly inhibited tumor growth. Therefore, the combination use of CD80 fusion protein and DDR1 inhibitor could become an effective tumor immunotherapy strategy, potentially benefiting a larger number of patients.

Key points

- *We successfully constructed, expressed, and purified the recombinant CD80-Fc fusion protein*
- *We demonstrated that CD80-Fc fusion protein has good safety and anti-tumor activity*
- *We demonstrated that using CD80-Fc fusion protein along with DDR1 inhibitor can significantly promote immune infiltration of T cells in tumor microenvironment and more strongly inhibit tumor growth*

Keywords CD80-Fc fusion protein · DDR1 · T cell costimulatory signals · Immune infiltration · Cancer immunotherapy

Introduction

Previous studies have pointed to two classical immune checkpoint pathways, one in which cytotoxic T-lymphocyte-associated protein 4 (CTLA-4) interacts with CD80 to limit the activation of initial T cell and the other in which programmed cell death protein 1 (PD-1) interacts with its ligand, programmed cell death 1 ligand 1 (PD-L1), in the tumor microenvironment to deplete effector T cells (Ribas and Wolchok 2018). Thus, blocking immune checkpoint signals can potentially enhance the anti-tumor immune response. Over the past few years, the US Food and Drug Administration (FDA) has approved ICIs for treating various solid tumor, with certain clinical efficacy (Huynh et al. 2021; Larkin et al. 2015; Xu et al. 2018). However, the majority of patients exhibit a low response rate or even develop resistance (Das and Johnson 2019; Lei et al. 2020). Hence, it is crucial to develop new strategies to improve the effectiveness of cancer immunotherapy.

CD80 is a transmembrane glycoprotein containing 254 amino acid residues, frequently expressed on various antigen-presenting cells (Bhatia et al. 2005). The

✉ Li Ye
lye@must.edu.mo

1 School of Pharmacy and Laboratory of Drug Discovery From Natural Resources and Industrialization, Macau University of Science and Technology, Macau SAR 999078, China

2 Department of Biological Medicines at School of Pharmacy, Fudan University, Shanghai 201100, China

3 Beijing Beyond Biotechnology Co., Ltd, Room 308, C Building, NO.18 Xihuannanlu Street, BDA, Beijing 100176, China

Published online: 07 February 2025

extracellular domain (ECD) of CD80 primarily includes an IgV domain and an IgC domain. And the IgV domain is mainly involved in binding to its receptors (Nagai and Azuma 2019). CD80 is a natural ligand of CD28 costimulatory molecule. During the immune response, CD28/CD80 costimulatory signal together with TCR/MHC signal activates T cells through mitogen-activated protein kinase (MAPK), nuclear factor kappa-B (NF-κB), and the calcium-calcineurin signaling pathways, which induce the secretion of various cytokines including interleukin-2 (IL-2), tumor necrosis factor-α (TNF-α), and interferon-γ (IFN-γ) (Boise et al. 1995; Snanoudj et al. 2007). In particular, various pieces of evidence indicate that PD-1-mediated immunosuppression is predominantly mediated by the costimulatory receptor CD28 (Hui et al. 2017). PD-1 in combination with PD-L1 will trigger the aggregation of Src homology-2-containing protein tyrosine phosphatase 2 (SHP2) and preferentially dephosphorylates CD28 cytoplasmic tail on T cells (Yokosuka et al. 2012). This blocks the transduction of CD28/CD80 costimulatory signal, thereby hindering T cell activation. Hence, the essence of PD-1-targeting immune checkpoint inhibitors is to alleviate its inhibition of CD28/CD80 costimulatory signaling, thereby reactivating the anti-tumor immune response (Kamphorst et al. 2017). An additional study confirmed this by showing that the efficacy of anti-PD-1 antibodies greatly decreased with the use of CD80 blocking antibodies (Ikemizu et al. 2000). Therefore, it is possible to achieve better anti-tumor effects by adding exogenous CD80 to provide sufficient costimulatory signals.

In addition, previous researches suggested that the interaction of CD80 and CTLA-4 could inhibit protein kinase B phosphorylation by activating the phosphatase PP2A5, leading to a decrease in cytokine secretion (Intlekofer and Thompson 2013; Krummel and Allison 1996; Parry et al. 2005). Notably, CD28 and CTLA-4 exhibit high homology, sharing the MYPPPY binding motif. However, CTLA-4 demonstrates a greater affinity for the ligand (Azuma 2019; Sansom 2000). When CD80 is bound by CTLA-4 rather than CD28, it effectively diminishes the costimulatory signals essential for the complete activation of T cells. This phenomenon is particularly notable within the tumor microenvironment, where tumor cells expressing low levels of CD80 tend to selectively interact with CTLA-4, thereby inhibiting T cell activation. Such interference is considered a strategic evasion tactic employed by tumors to evade immune surveillance (Vackova et al. 2021).

Discoidin domain receptor 1 (DDR1), as a receptor for collagen, operates with tyrosine kinase activity. Structurally, it mainly comprises an extracellular domain, a transmembrane domain, and an intracellular kinase domain (Gao et al. 2021). By engaging with various extracellular matrix (ECM) components, DDR1 regulates many cellular processes like adhesion, migration, and proliferation (Leitinger 2014; Valiathan et al. 2012). Researches have shown a significant upregulation of DDR1 expression across diverse cancer types, including ovarian, lung, and brain cancers. This heightened expression correlates with aggressive malignant behaviors, including tumor progression, invasion, and metastasis (Ambrogio et al. 2016). Additionally, a recent study indicates that DDR1 may be one of the crucial proteins that prevent immune cells from approaching tumors. The ECD of DDR1 transforms the ECM into a highly ordered state by enhancing the alignment of collagen fibers, which in turn prevents immune cell infiltration (Sun et al. 2021). In subsequent studies, it was found that knocking out DDR1 in mice with triple-negative breast cancer could promote T cell infiltration and inhibit tumor growth. The absence of DDR1 correlated with reduced and abbreviated collagen fibrillation at the tumor periphery, heightened the presence of $CD8^+$ and $CD4^+$ T cells within the tumor microenvironment, and facilitated IFN-γ production (Sun et al. 2021). These are all allowed immune cells to effectively execute their tumor-killing activity. In our previous published article, we identified a noteworthy association between DDR1 and immune cell infiltration in gastric cancer (Wang et al. 2022). Additionally, a separate study has also indicated a robust association between low CD80 level and unfavorable overall survival (OS) and disease-free survival (DFS) among individuals diagnosed with gastric cancer (Feng et al. 2019). Therefore, we tried to use CD80-Fc fusion protein and DDR1 inhibitors for treating gastric cancer, in order to make more activated T cells infiltrate into the tumor and play an effective anti-tumor activity. This may provide new potential for immunotherapy of gastric cancer.

Materials and methods

Cells and mice

MC38 and LLC cell lines were obtained from the Cell Bank of Chinese Academy of Sciences (Shanghai, China). These cells were cultured in DMEM medium supplemented with 10% fetal bovine serum (Gibco) and 1% penicillin–streptomycin solution (Beyotime). Incubation of cells was carried out in incubators set to maintain 5% CO_2 and a temperature of 37 °C. None of the cells was infected with mycoplasma. Male C57BL/6 mice were obtained from BK Lab Animal Ltd. (Shanghai, China).

Construction, expression, and purification of CD80-Fc

The gene fragment encoding the mouse CD80 extracellular domain (GenBank accession no. AAI31960.1) was inserted into the N-terminus of IgG2a Fc fragment (GenBank

accession no. AAB59660.1), and then, the encoded nucleotide of mouse CD80-Fc (mCD80-Fc, GenBank accession no. OR036994) was ligated to a high efficiency glutamine synthase expression vector with double expression box (CN104195173B, Beijing Beyond Biotechnology Company) by restriction enzymes *Eco*RI and *Xho*I. The plasmid of mCD80-Fc fusion protein was synthesized by Jierui bioengineering company. After the sequence was correct, the plasmid was used to express the target protein. 293F cells in the culture medium were centrifuged to obtain cell precipitation, and then, the cells were resuspended by using a fresh serum-free CD293 culture medium. Next, we took 100 mL of the cell suspension and placed it in a shaking flask. Two hundred fifty micrograms of recombinant expression vector plasmid DNA containing the target gene and 500 μg of polyethyleneimine (PEI) were added to the serum-free CD293 culture medium and then remained for 8 min. We next added the PEI/DNA mixture to the previous shaker and gently mixed them. The cells were placed on a shaking bed at 37 °C with 5% CO_2, and the supernatant from the culture was harvested after 5 days. Subsequently, the acquired supernatant was purified by affinity chromatography. Analysis of the molecular weight of the mCD80-Fc was conducted using 10% sodium dodecyl sulfate polyacrylamide gel electrophoresis (SDS-PAGE).

The term "hu-CD80-Fc fusion protein" denotes the fusion of the ECD of human CD80 with the N-terminal segment of the Fc region of human IgG4. This specific expression and purification process was described above.

Binding affinity measurement

Binding affinity was detected using a Biacore T200 system (GE Healthcare) outfitted with a His capture chip from JOINN Biologics. Mouse CTLA-4 (0.5 μg/mL, CT4-M52H5, ACRO Biosystems), PD-L1 (1 μg/mL, PD1-M5220, ACRO Biosystems), and CD28 (2 μg/mL, CD8-M52H6, ACRO Biosystems) proteins with His tags were first flowed across the chip surface so that they were respectively captured by His antibodies on the chip surface. Subsequently, different gradient concentrations of the fusion protein were separately flowed across the chip surface at a flow rate of 30 μL/min. All combined and elution curves were recorded. Then, we analyzed the data by using the Biacore T200 Evaluation software (version 2.0.2). Various parameters including the binding rate (ka), the dissociation rate (kd), and the affinity (K_D) were calculated.

Tumor models and treatments

MC38 or LLC cells were cultured to logarithmic growth phase, digested with trypsin (Beyotime), and resuspended in 1 × PBS solution. For allograft tumor models, mice anesthetized by inhalation of isoflurane were injected subcutaneously with 200 μL 5×10^6/mL or 5×10^5/mL cell suspension to produce tumors. Upon reaching tumor volumes of around 100–150 mm^3, all mice were allocated randomly to one of three categories: control group (PBS), CD80-Fc treatment group (1.34 or 3.34 mg/kg), and anti-PD-1 antibody treatment group (2 or 5 mg/kg, Univ). Mice were treated according to the specified drug concentration once every 3 days. Before each administration, the measurement of the body weight and tumor volume was performed. After the treatment period, mice were euthanized for research purposes. Tumors and major organs were collected and studied. Approval for all animal experimentation was obtained from the Laboratory Animal Ethics Committee of the School of Pharmacy, Fudan University.

In vivo blocking assay

The sphingosine-1-phosphate (S1P) receptor agonist FTY720 (SML0700, Sigma) which inhibits lymphocyte egress from lymph nodes and restricts the migration of activated T cells into tumors was used in the in vivo blocking assay (Chiba 2005). Here, MC38 cells were cultured to logarithmic growth stage in incubators set to maintain 5% CO_2 and a temperature of 37 °C. Following trypsin digestion (Beyotime), cells were suspended in a 1 × PBS solution. These cell suspensions were inoculated subcutaneously into the right subcostal side of 6-week-old male C57BL/6 mice, with 200 μL injected into each one. Upon reaching a tumor volume of about 100–150 mm^3, all mice were randomly divided and were treated with PBS, 1.34 mg/kg mCD80-Fc fusion protein, 1.25 mg/kg FTY720, and a combination of mCD80-Fc and FTY720, respectively. The frequency of administration was once every 3 days, while FTY720 was administered every other day throughout the duration. Before each administration, measurements of the mice's body weight and tumor volume were taken, while their health and diet were observed. At the conclusion of the treatments, the mice were euthanized for research purposes, and both tumors and major organs were collected and studied. Approval for all animal experiments was granted by the Laboratory Animal Ethics Committee of the School of Pharmacy, Fudan University.

PBMCs-PDX gastric cancer models and treatment

After collecting fresh gastric cancer tissues from patients, we immediately minced them into small pieces of approximately 1 mm^3 volume using forceps and scissors under aseptic conditions. NCG mice (GemPharmatech) were anesthetized with an isoflurane anesthesia machine. We then made a 1-cm incision on both sides of the back in mice with sterile scissors and implanted tumor pieces into

them. After the surgery, the mice were placed gently in an empty cage and their condition was closely monitored. Once the tumor diameter reached 1.5 cm, the euthanasia of the mice was performed. The new NCG mice were then implanted with post-dissection tumors for passage.

Whole blood from healthy people was collected into the anticoagulant tubes. Human peripheral blood mononuclear cells (PBMCs) were isolated using human lymphocyte isolation solution following the manufacturer's instruction. 1×10^6 human PBMCs were transplanted into tumor-bearing mice through tail vein injection. Once the tumor volume reached 100–150 mm^3, the mice were randomly divided into four groups: control group (PBS), hu-CD80-Fc treatment group (3.34 mg/kg), VU6015929 (a DDR1 inhibitor, CAS:2,442,597–56-8, AbMole) treatment group (6 mg/kg), and the combination treatment group (3.34 mg/kg hu-CD80-Fc and 6 mg/kg VU6015929). Treatments were administered once every 3 days, with continuous monitoring and recording of the mice's weight and tumor volume. After completion of the treatment regimen, the mice were euthanized, and both tumors and major organs were harvested for further analysis.

Immunohistochemical staining

Four percent paraformaldehyde (Servicebio) was used to fix the tumors and spleens from mice. The samples underwent embedding in paraffin, following which they were sliced into sections with a thickness of 5 μm. Among them, the position of mouse tumor section came from inside the tumors. Then, they were incubated with primary antibodies, including rabbit anti-mouse CD3 (GB111337, 1:700, Servicebio), rabbit anti-mouse CD4 (GB13064-2, 1:400, Servicebio), rabbit anti-mouse CD8 (GB13429, 1:400, Servicebio), rabbit anti-human CD3 (GB111337, 1:700, Servicebio), rabbit anti-human CD4 (GB13064-2, 1:400, Servicebio), and rabbit anti-human CD8 (GB13429, 1:400, Servicebio) antibodies. Fluorescein isothiocyanate-labeled goat anti-rabbit IgG (H + L) (GB23303, 1:200, Servicebio) was utilized as a secondary antibody. Imaging was conducted using the VS200 full slide scanner (Olympus Corporation). There were six samples in each group, and five random regions were selected for each sample for analysis. The percentage of target positive was evaluated by IHC profiler of ImageJ software. Data analysis was performed using GraphPad Prism 8 software (San Diego).

H-E staining

The H-E staining of tumors and organs was conducted according to conventional protocol. In detail, tumor tissues were collected from mice, fixed in 4% paraformaldehyde (Servicebio), then embedded with paraffin. The section of each sample was stained with hematoxylin solution (ZSGB-BIO) for 5 min. The sections were repeatedly soaked 5 times in 1% acidic ethanol and stained with eosin solution (ZSGB-BIO) for 3 min. Following dehydration in alcohol and clearing in xylene, slides were scanned with a VS200 full slide scanner (Olympus Corporation).

Detection of serum cytokines

After the mice were sacrificed, whole blood was collected and centrifuged at 4 °C. Following the manufacturer's guidelines, the upper serum was collected and measured cytokine concentration by INF-γ ELISA kit (EK280-96, MULTI SCIENCES) and TNF-α ELISA kit (EK282-96, MULTI SCIENCES). Triplicate testing was carried out for each condition, and subsequent data analysis was conducted using GraphPad Prism 8 software from San Diego.

UCSC Xena

UCSC Xena (https://xena.ucsc.edu) is an online platform for genomic and transcriptomic data analysis, which integrates large-scale genomic and transcriptomic datasets from multiple public data sources (Goldman et al. 2020). We employed UCSC Xena to evaluate the expression levels of PD-1, PD-L1, CD28, CTLA-4, and DDR1 in stomach adenocarcinoma (STAD). Two datasets including the GDC TCGA Stomach Cancer dataset and the TCGA Stomach Cancer dataset were used for analysis. Finally, the data was visualized using the box plots and the statistical difference was performed using Welch's test.

Analysis of clinical samples from gastric cancer patients

All tumor tissues from gastric cancer patient were obtained from the Changhai Hospital of Shanghai (Shanghai, China). Written informed consent was obtained from each patient participating in all trials, and the protocols were approved by the Clinical Research Ethics Committee of Changhai Hospital (CREC: check-2021–119). The samples underwent fixation in 4% paraformaldehyde, followed by paraffin embedding and excision into 5-μm sections. After that, they were subjected to incubation with primary antibodies, which included rabbit anti-human DDR1 antibody (GB111290, 1:1000, Servicebio), rabbit anti-human CTLA-4 antibody (T57117S, 1:200, ABMART), and rabbit anti-human PD-L1 antibody (MH68942S, 1:200, ABMART). Fluorescein isothiocyanate-labeled goat anti-rabbit IgG (V + L) (GB23303, 1:200, Servicebio) served as the secondary antibody. All sections were visualized using an Olympus VS200 full slide scanner. Data analysis was performed using GraphPad Prism 8 software (San Diego).

Statistical analysis

Unless otherwise noted, data analysis for all experiments was conducted using GraphPad Prism 8 software, with results presented as mean ± SD. Statistical significance was denoted by asterisks, with significance deemed if the *P* value was < 0.05.

Results

Construction and expression of human and mouse CD80-Fc fusion protein

To simplify the purification process and extend in vivo half-life, we designed a soluble CD80-Fc fusion protein (hu-CD80-Fc) by fusing human CD80 ECD with Fc domain of immunoglobulin (Fig. 1A). Then, the expression plasmid of recombinant fusion protein was constructed using high expression vector, and the target protein was expressed by transient transfection (Fig. 1B). By using the 293F cell line, we expressed the fusion protein and purified it using affinity chromatography. After purification, further identification was performed by using reduced and non-reduced SDS-PAGE. As shown in Fig. 1C, most irrelevant proteins were removed after purification and a single fusion protein was obtained. In addition, the molecular weight (65 kDa) measured under reduced condition was slightly higher than the theoretical value (50.2 kDa). We speculated that this might be related to the existence of glycosylation in the eukaryotic expression system, which increased the apparent molecular weight of the protein. Subsequently, ELISA assay determined the binding affinity of hu-CD80-Fc against CD28, CTLA-4, and PD-L1. Optical density measurement indicated that hu-CD80-Fc could specifically bind recombinant human CD28, CTLA-4, and PD-L1 proteins (Fig. 1D). The EC50 values of hu-CD80-Fc against CD28, PD-L1, and CTLA-4 were 6.231, 5.295, and 5.235 μg/mL, respectively. These results suggested that hu-CD80-Fc had an appropriate affinity against the targets. Furthermore, we measured the affinity of hu-CD80-Fc against the Fc receptor (FcR) and obtained EC50 values of 151.5 μg/mL (Fig. 1D).

Moreover, in order to verify the efficacy more conveniently, we also constructed a murine-derived CD80-Fc fusion protein. We designed the mCD80-Fc fusion protein by fusing the ECD of mouse CD80 with the IgG Fc segment (Fig. S1A). In the same way that hu-CD80-Fc fusion protein was expressed, the optimized nucleotide sequences of mCD80-Fc were utilized to construct

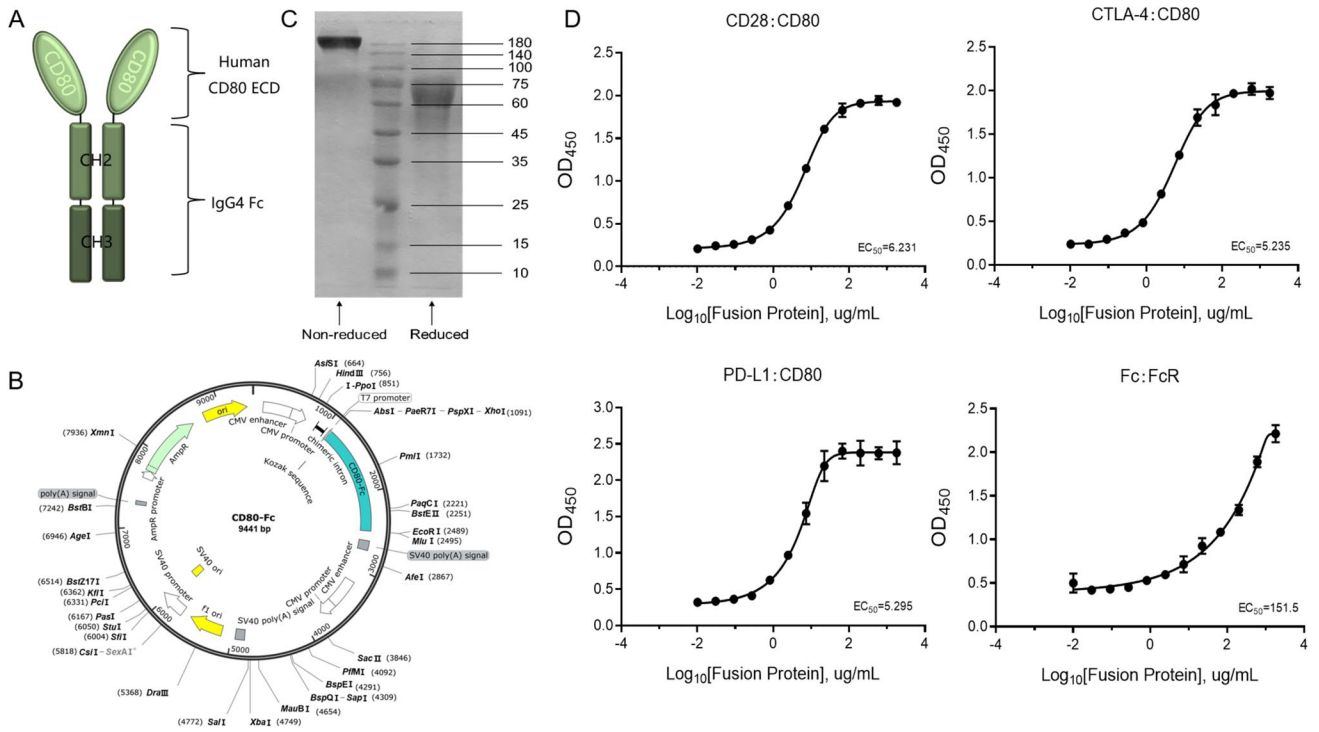

Fig. 1 Construction and expression of human CD80-Fc fusion protein. **A** The diagram of hu-CD80-Fc. **B** Schematic of eukaryotic expression vector. **C** The SDS-PAGE analysis of hu-CD80-Fc under either reducing or non-reducing conditions. **D** Sandwich ELISA assay measured the binding affinity of hu-CD80-Fc for recombinant human CD28, CTLA-4, PD-L1, and FcR proteins. For EC_{50} determination, protein concentrations and OD_{450} values were log transformed before analysis and fit by using GraphPad Prism 8 software

the expression vector, and the protein was transiently expressed using 293F cells. Following purification, mCD80-Fc was evaluated through reduced and non-reduced SDS-PAGE electrophoresis (Fig. S1B). The protein molecule measured under reducing conditions was 65 kDa, slightly higher than the theoretical value (50 kDa). It is also possible that this difference could be attributed to glycosylation in the eukaryotic expression system. After determining the stable expression of mCD80-Fc, we used the Biacore to determine its binding affinity to three targets. By using the Biacore T200 Evaluation Software to fit the results, we found that the K_D values of mCD80-Fc for CTLA-4, CD28, and PD-L1 were 4.209×10^{-3}, 2.487, and 13.36 μM, respectively, under the experimental conditions (Fig. S2).

CD80-Fc fusion protein has good anti-tumor activity in vivo

To assess the in vivo anti-tumor activity of CD80-Fc, we first transplanted MC38 cells into C57BL/6 mice by subcutaneous injection to construct an allograft tumor model, which is highly immunogenic. When the tumor volumes reached about 100 mm^3, the mice were intraperitoneally injected with PBS, mCD80-Fc, and anti-mPD-1 antibody once every 3 days (four injections in total). The changes in tumor size with PBS, mCD80-Fc, or anti-mPD-1 antibody treatment were checked every 3 days, showing an outstanding therapeutic effect of mCD80-Fc fusion protein (Fig. S3). As depicted in Fig. 2A, compared with the control group, mCD80-Fc fusion protein and equimolar dose of anti-mPD-1 antibody both exhibited significant and comparable tumor suppressive effects. At day 19, the volumes of the mCD80-Fc-treated and anti-mPD-1-treated tumor were 1186.15 ± 635.41 mm^3 and 1316.52 ± 464.03 mm^3, which was 2.27- and 2.05-fold smaller than PBS-treated ones, respectively. During the therapeutic procedures, none of the subject mice which were injected with mCD80-Fc suffered from serious systemic adverse events or elicited meaningful weight loss (Fig. 2B). Subsequently, mice were euthanized and dissected. Weighing and statistical analysis were performed on the residual tumors. In comparison to the control group, the tumor weight of the mice treated with mCD80-Fc fusion protein and anti-mPD-1 antibody was reduced by 1.59 ± 0.21 g ($P < 0.0001$) and 1.46 ± 0.21 g ($P < 0.0001$), respectively (Fig. 2C). These results suggested that mCD80-Fc had a significant anti-tumor effect in vivo.

The significant anti-tumor activity of mCD80-Fc led us to further explore its potency in controlling poorly immunogenic

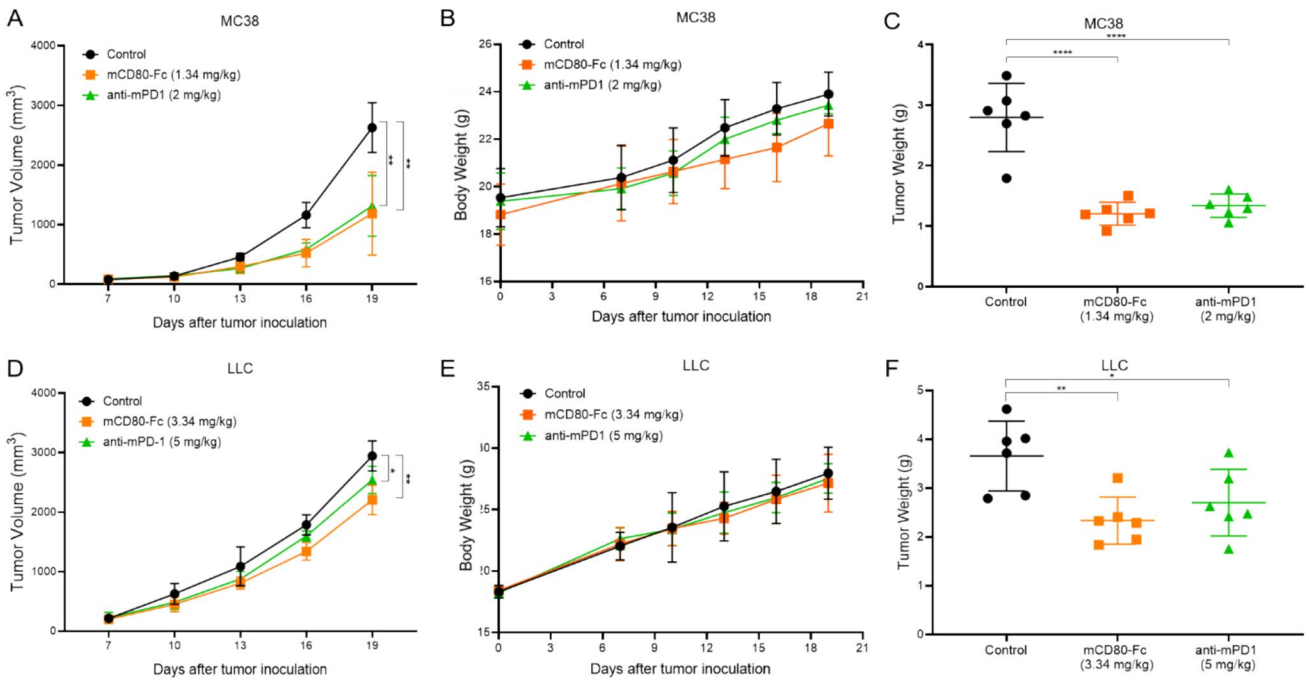

Fig. 2 CD80-Fc fusion protein has good anti-tumor activity in vivo. **A** MC38 tumor growth curves of each group treated with 10 mL/kg PBS ($n = 6$), 1.34 mg/kg mCD80-Fc ($n = 6$), and 2 mg/kg anti-mPD-1 antibody ($n = 6$), respectively. **B** Body weight growth curves of MC38 tumor-bearing mice ($n = 6$). **C** The weight of the residual MC38 tumors in different groups ($n = 6$). **D** LLC tumor growth curves of each group treated with 10 mL/kg PBS ($n = 6$), 3.34 mg/kg mCD80-Fc ($n = 6$), and 5 mg/kg anti-mPD-1 antibody ($n = 6$), respectively. **E** Body weight growth curves of LLC tumor-bearing mice ($n = 6$). **F** The weight of the residual LLC tumors in different groups ($n = 6$). The data were presented as mean ± SD, with significance indicated by the following symbols: $^*P < 0.05$, $^{**}P < 0.01$, $^{***}P < 0.001$, $^{****}P < 0.0001$

and cold tumor model. Here, we performed similar experiment using LLC tumor-bearing mice. Changes in tumor size with PBS, mCD80-Fc, and anti-mPD-1 antibodies treatment were measured every 3 days after initiation of administration (Fig. S4). Once again, we observed that mCD80-Fc fusion protein could significantly control tumor growth and was more effective than anti-mPD-1 antibody at equimolar dose (Fig. 2D). The volume of the mCD80-Fc-treated tumor was 1288.90 ± 109.35 mm^3 at day 19, which was 1.39- and 1.16-fold smaller than PBS- and anti-mPD1-treated ones, respectively. During the therapeutic procedures, none of the subject mice which were injected with mCD80-Fc or anti-mPD-1 antibody suffered from serious systemic adverse events or elicited meaningful weight loss (Fig. 2E). Finally, the residual tumors were weighed and analyzed statistically. In comparison to the control group, mice treated with mCD80-Fc exhibited a reduction in tumor weight by 1.32 ± 0.37 g ($P < 0.01$), while those treated with the anti-mPD-1 antibody showed a reduction by 0.96 ± 0.37 g ($P < 0.05$) (Fig. 2F). In summary, mCD80-Fc had a promising anti-tumor effect in vivo.

The degree of immune infiltration affects the efficacy of CD80-Fc fusion protein

Given that CD80 is a pivotal costimulatory molecule in T cell activation, immunohistochemical staining was performed to analyze T cell presence within tumor tissue. The results showed a significant increase in the number of effector CD8$^+$ T cells in both MC38 and LLC tumors (Fig. 3A–D). This suggests that CD80-Fc effectively activates T cells and plays an anti-tumor role. However, we observed that the anti-tumor effect of CD80-Fc in LLC cold tumor, as well as cytotoxic T lymphocyte infiltration level, was not as pronounced as in the MC38 tumors. This prompted us to investigate whether effector T cell infiltration in tumor might influence the efficacy of the CD80-Fc fusion protein. Hence, we used blocking assays in vivo for validation. FTY720, acting as an agonist of the sphingosine 1-phosphate (S1P) receptor, impedes the migration of primary or effector lymphocytes from lymph nodes to circulating and peripheral tissues. It also restricts the migration of

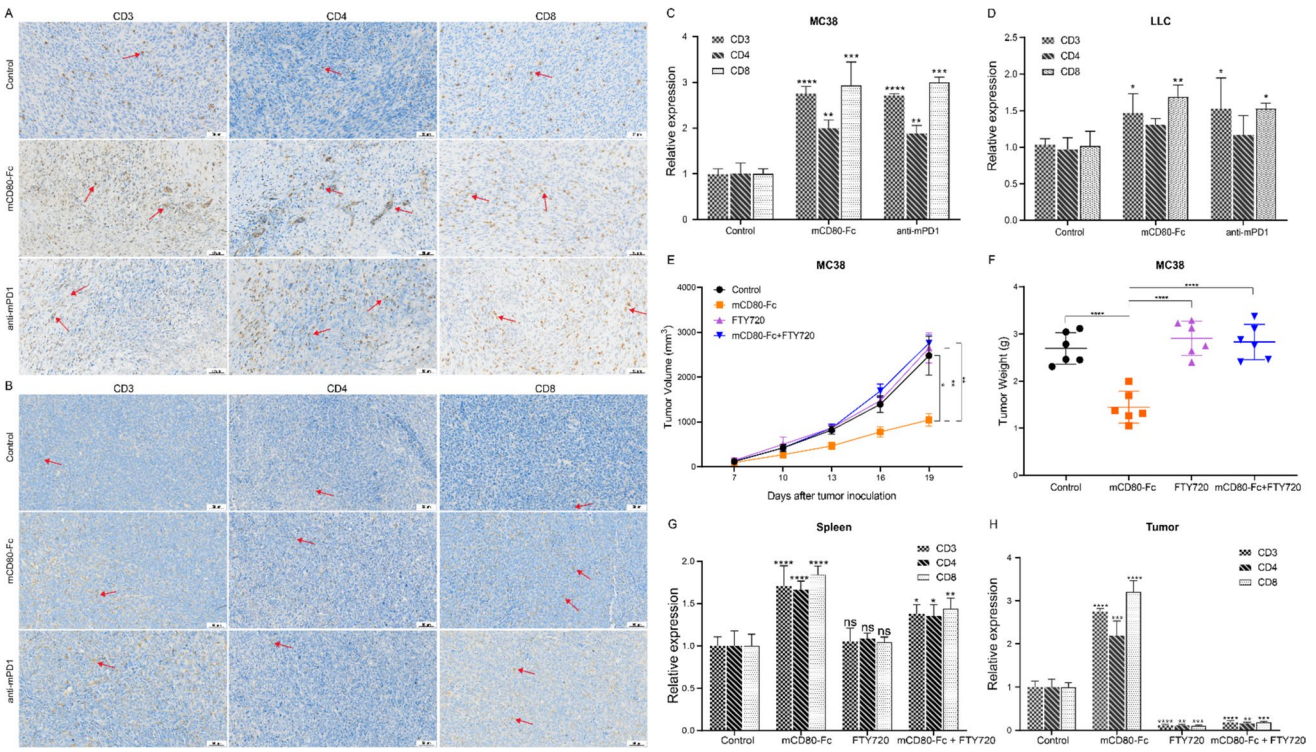

Fig. 3 The degree of immune infiltration affects the efficacy of CD80-Fc fusion protein. **A** Immunohistochemical staining analysis was conducted on CD3, CD4, and CD8 in the MC38 tumors. Images were photographed by VS200 full slide scanner. **B** Immunohistochemical staining analysis of CD3, CD4, and CD8 in the LLC tumors. **C** Statistical results of CD3$^+$, CD4$^+$, and CD8$^+$ T cells in the MC38 tumors. The cells that expressed CD3, CD4, and CD8 (brown staining) were counted with Image J software. **D** Statistical results of CD3$^+$, CD4$^+$, and CD8.$^+$ T cells in the LLC tumors. **E** Tumor growth curves of each group treated with PBS (10 mL/kg), mCD80-Fc (1.34 mg/kg), FTY720 (1.25 mg/kg), and mCD80-Fc in combination with FTY720. **F** The weight of the residual MC38 tumors ($n = 6$). **G** Immunohistochemical staining analysis of CD3, CD4, and CD8 in the spleens. **H** Immunohistochemical staining analysis of CD3, CD4, and CD8 in the tumors. The data were presented as mean ± SD, with significance indicated by the following symbols: *$P < 0.05$, **$P < 0.01$, ***$P < 0.001$, ****$P < 0.0001$

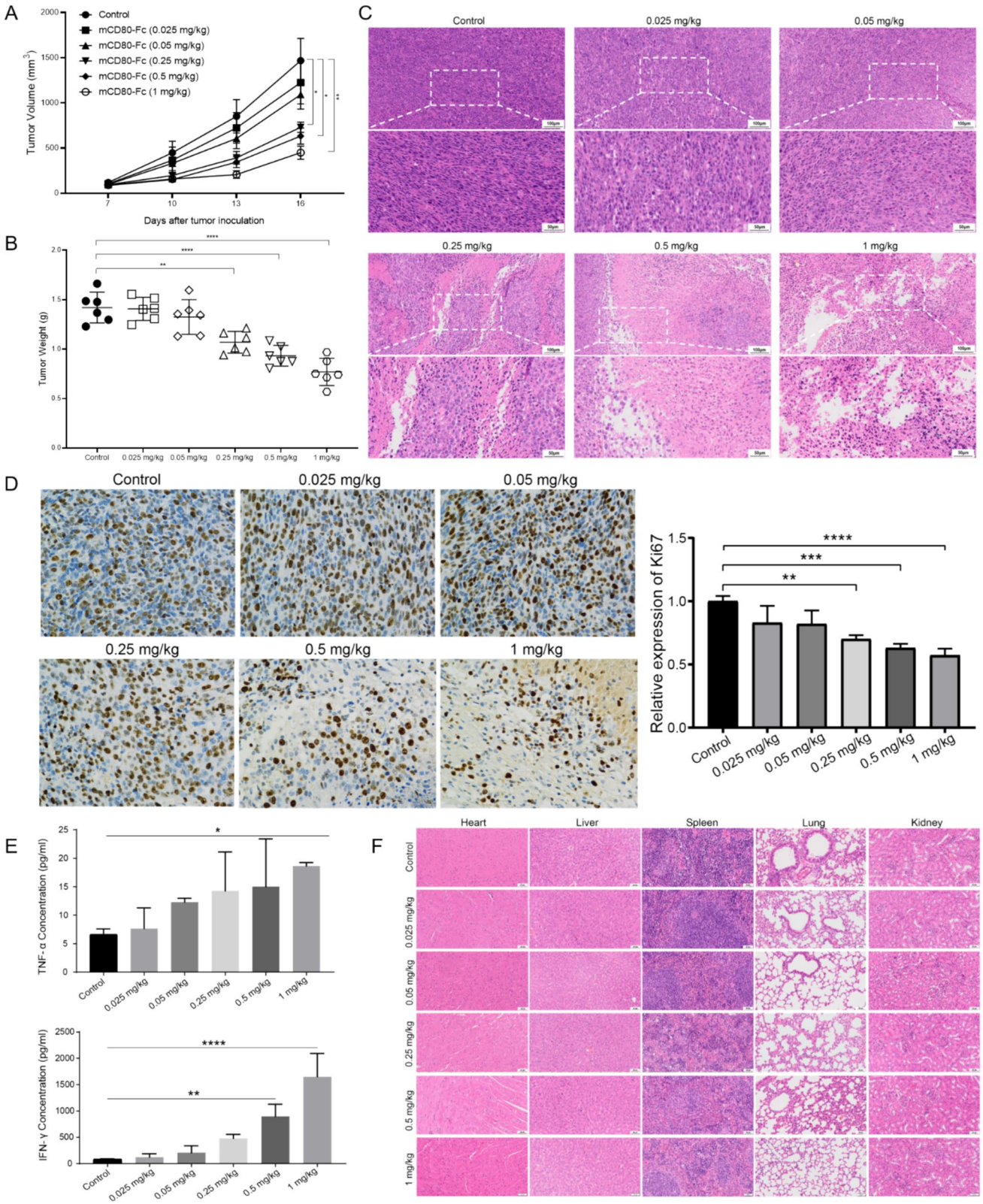

activated T cells into tumors (Chiba 2005). We first constructed the MC38 allograft tumor model using C57BL/6 mice. The mice in each group were treated separately after randomization. On the 19th day of treatment, tumor growth of mice in the mCD80-Fc-treated group was significantly inhibited, while tumor growth of mice in the FTY720 group

◂**Fig. 4** CD80-Fc fusion protein has good safety and dose dependence. **A** Mice were administrated intraperitoneally with 10 mL/kg PBS and 0.025, 0.05, 0.25, 0.5, and 1 mg/kg mCD80-Fc, respectively. Tumor growth curve of six groups ($n=6$). **B** The weight of the residual MC38 tumors in different groups ($n=6$). **C** Representative microphotographs of tumor H-E staining in mice treated with different doses of mCD80-Fc fusion protein. Magnification: ×100, ×200. Scale bar = 100 μm, 50 μm. **D** Representative microphotographs of the tumors stained with anti-Ki67 antibody (brown staining). Scale bar = 100 μm. Images J software was used to count tumor cells that expressed Ki67. **E** Detection of TNF-α and IFN-γ concentrations. **F** H-E staining analysis of viscera in mice. Magnification: ×200. All pictures were photographed by VS200 full slide scanner. All data were represented as mean ± SD (*$P<0.05$, **$P<0.01$, ***$P<0.001$, ****$P<0.0001$)

was consistent with that of the control group (Fig. 3E). However, combining FTY720 with mCD80-Fc abolished anti-tumor efficacy of mCD80-Fc. These results corresponded to the results of tumor weight in mice (Fig. 3F). In addition, during the therapeutic procedures, none of the subject mice suffered from serious systemic adverse events or elicited meaningful weight loss (Fig. S5).

To further analyze the above result, immunohistochemical staining was performed on both tumors and spleens tissues, respectively (Fig. S6 and S7). The results showed that administration of FTY720 alone did not influence the number of spleen T cells but effectively blocked the entry of T cells into the tumor (Fig. 3G and H). In contrast, a significant increase of T cells in the spleen was observed after administration of mCD80-Fc alone, indicating that mCD80-Fc fusion protein effectively activated T cells (Fig. 3G). At the same time, the number of T cells in mCD80-Fc-treated tumor also increased significantly, indicating that activated T cells infiltrated the tumor (Fig. 3H). However, when FTY720 was combined with mCD80-Fc, there was an increase in T cells within the spleen but a significant decrease in T cells within the tumor. Combined with tumor growth curves, these results suggest that CD80-Fc fusion protein can activate T cells effectively, and the activated T cells need to infiltrate into the tumor to exert the tumor-killing activity. Therefore, we speculated that the degree of immune infiltration would affect the in vivo efficacy of CD80-Fc fusion protein. This also provides us with a direction for the combination drug strategy in the subsequent research.

CD80-Fc fusion protein has good safety and dose dependence

We next tested the anti-tumor effect of CD80-Fc by a range of doses to determine the minimum effective schedule. Mice bearing established MC38 tumors were treated with different doses of mCD80-Fc (0.025, 0.05, 0.25, 0.5, 1 mg/kg) by intraperitoneal injection. In different groups of mice, tumor volume and body weight were individually recorded. At the end of administration, we found that tumor growth was significantly inhibited in mice treated with 0.25, 0.5, and 1 mg/kg mCD80-Fc fusion protein (Fig. 4A). In contrast to the control group, mice treated with mCD80-Fc fusion protein at doses of 0.25, 0.5, and 1 mg/kg exhibited reductions in tumor weight by 1.16 ± 0.25 g ($P<0.05$), 1.27 ± 0.25 g ($P<0.05$), and 1.77 ± 0.25 g ($P<0.01$), respectively (Fig. 4B). The above results demonstrated that mCD80-Fc still had effective anti-tumor activity at doses as low as 0.25 mg/kg, which could greatly improve the safety of fusion protein used. Subsequently, H-E staining and Ki67 immunohistochemical staining of the residual tumor tissue were performed. In H-E staining, more local necrosis of tumors was observed with the dose of mCD80-Fc increased (Fig. 4C). In Ki67 immunohistochemistry staining, the relative expression of Ki67 was getting lower with increasing dose, which indicated that the proliferation of tumor cells was getting weaker (Fig. 4D). In conclusion, these results demonstrated that CD80-Fc fusion protein inhibited tumor growth in a dose-dependent manner.

It was reported that the anti-CD28 monoclonal antibody TGN1412 caused severe cytokine release syndrome (Suntharalingam et al. 2006). Therefore, considering the activating effect of CD80, we further evaluated the safety of CD80-Fc fusion protein. During the therapeutic procedures, none of the subject mice suffered from serious systemic adverse events or elicited meaningful weight loss (Fig. S8). The concentration of TNF-α and IFN-γ in mouse serum after drug administration was measured. mCD80-Fc fusion protein increased the release of TNF-α and IFN-γ, but there were no symptoms associated with CRS (Fig. 4E). Moreover, H-E staining was used for pathological analysis of vital organs in mice. There were no obvious pathological damages of major organs across all groups (Fig. 4F). To sum up, CD80-Fc has a good safety profile. However, further evaluation is warranted to assess the safety of higher doses of the CD80-Fc fusion protein.

hu-CD80-Fc combined with DDR1 inhibitor effectively inhibits tumor growth and promotes immune infiltration

The above research discovered that the degree of immune infiltration could affect the efficacy of CD80-Fc fusion protein. Additionally, in our previously published article, we identified elevated DDR1 expression in gastric cancer, which was correlated with unfavorable prognosis and inadequate immune infiltration based on database analysis (Wang et al. 2022). Therefore, we attempted to treat gastric cancer using a combination of hu-CD80-Fc and DDR1 inhibitor with the aim of achieving a stronger anti-tumor effect. To achieve this, we

constructed a PBMCs-PDX model of gastric cancer in NCG mice for further investigation. Considering the expression level of DDR1 in the PBMCs-PDX mouse model, we also performed immunohistochemical staining for DDR1 on the tumor tissues transplanted into the mice. The results showed a notably elevated expression of DDR1 in the tumor tissues of our mouse model, which could be used for subsequent in vivo pharmacodynamics experiments (Fig. S9). After the start of administration, changes in tumor size were measured every 3 days in each group of mice. As is shown in Fig. 5A, the combined administration of hu-CD80-Fc and the DDR1 inhibitor VU6015929 markedly suppressed tumor progression compared to monotherapy. The tumor volume of hu-CD80-Fc combined with VU6015929 treatment was 156.12 ± 37.06 mm^3 after 15 days of medication, which was 5.35-, 4.59-, and 4.81-fold smaller than PBS-, hu-CD80-Fc-, and VU6015929-treated ones, respectively. In addition, no serious systemic adverse events or elicited meaningful weight loss occurred during treatment in mice in the combination treatment group (Fig. S10). Further, we dissected the mice, and their residual tumors were analyzed statistically. The findings revealed that, in comparison to the control group, the tumor weights of mice in the hu-CD80-Fc treatment group, VU6015929 treatment group, and combined treatment group were reduced by 0.61 ± 0.08 g ($P < 0.001$), 0.27 ± 0.08 g ($P < 0.05$), and 0.90 ± 0.08 g ($P < 0.0001$), respectively (Fig. 5B). These results suggested that the combination of hu-CD80-Fc and VU6015929 had significant anti-tumor efficacy in vivo.

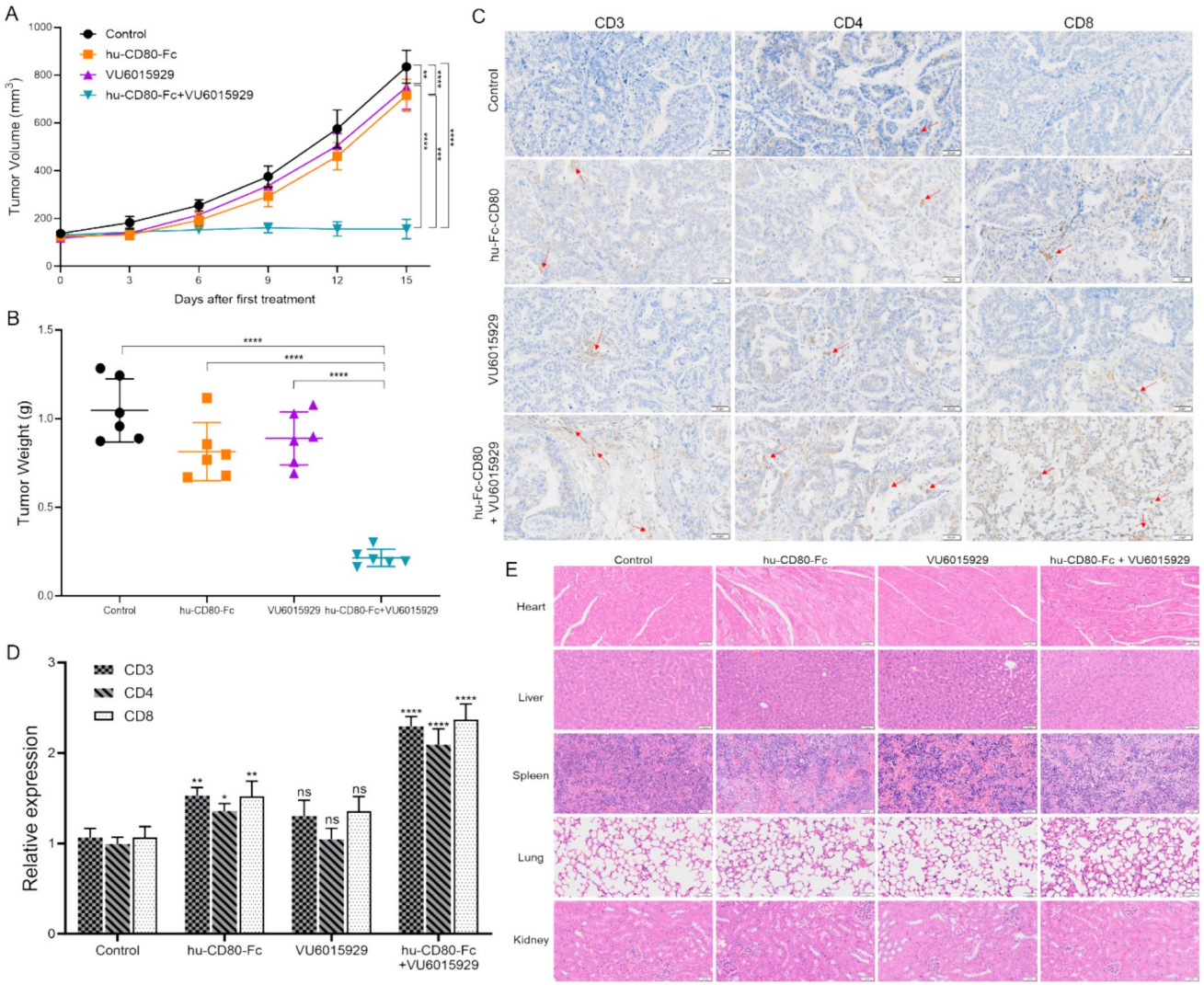

Fig. 5 hu-CD80-Fc combined with DDR1 inhibitor effectively inhibits its tumor growth and promotes immune infiltration. **A** Tumor volume growth of different groups ($n = 6$). **B** The weights of the residual tumors after the treatment ($n = 6$). **C** Immunohistochemical staining analysis of $CD3^+$, $CD4^+$, and $CD8^+$ T cells in the tumors. Magnification: × 200. **D** Statistical results of $CD3^+$, $CD4^+$, and $CD8^+$ T cells in the tumors. The cells that expressed CD3, CD4, and CD8 (brown staining) were counted with Image J software. **E** H-E staining analysis in mice. All pictures were photographed by an Olympus VS200 full slide scanner

To delve deeper into the impact of the combination on T cells, we performed immunohistochemical staining analysis on the tumor tissues. Statistical results indicated a notable augmentation in the T cell infiltration when using the combination use of hu-CD80-Fc fusion protein and DDR1 inhibitor (Fig. 5C and D). These findings suggested that hu-Fc-CD80 effectively activated T cells and increased the infiltration when combined with DDR1 inhibitor. Subsequently, H-E staining was used for pathological analysis of vital organs in mice. No significant pathological damage was detected in the administration groups (Fig. 5E). Our results indicated that the combination use of CD80-Fc and DDR1 inhibitor had the potential as a novel immunotherapy strategy for gastric cancer, potentially benefiting a broader range of patients.

Significant overexpression of CTLA-4, PD-L1, and DDR1 in the gastric cancer

In order to investigate the possibility of combining CD80-Fc and DDR1 inhibitor in the clinical treatment, we finally analyzed both database and clinical samples of gastric cancer patients. Initially, we assessed the mRNA expression levels of PD-L1, PD-1, CD28, CTLA-4, and DDR1 in gastric cancer using RNA-seq data from the UCSC Xena database. Compared with normal tissues, mRNA expression levels of PD-L1, DDR1, and CTLA-4 exhibited significant increases in the gastric cancer, while the expression of CD28 and PD-1 showed no significant difference (Fig. 6A and S11). In particular, the mRNA expression of DDR1 notably surpassed that of the other genes. Then, clinical samples from 20 patients with gastric cancer were collected and subjected to immunohistochemical staining analysis. Results depicted elevated expression levels of CTLA-4, PD-L1, and DDR1 in gastric cancer in comparison to normal tissues (Fig. 6B). These results indicated that inhibitory signals were enhanced and the costimulatory signal was insufficient in gastric cancer, consequently restraining T cell anti-tumor response. Simultaneously, DDR1 high expression in gastric cancer impeded immune cell infiltration. Therefore, the combined administration of recombinant CD80 fusion protein and DDR1 inhibitor holds promise as an innovative approach for treating gastric cancer. On the one hand, the fusion protein enhances T cell responses through dual mechanisms: activating the CD28/CD80 costimulatory signal while simultaneously inhibiting PD-L1 and CTLA-4 coinhibitory signals. On the other hand, inhibition of DDR1 promotes tumor immune infiltration and synergistically enhances anti-tumor effect.

Discussion

CD80, which belongs to type I transmembrane protein, typically appears as a dimer on cell surfaces (Bhatia et al. 2005; Liu and Zang 2019; Nagai and Azuma 2019). CD80 possesses the capability to interact with CD28, thereby generating a costimulatory signal that facilitates activation, proliferation, and differentiation of T cells. Conversely, when CTLA-4 binds with CD80 on antigen-presenting cell membranes, it triggers an inhibitory signal that suppresses the activation of T cells. Some researchers highlighted that soluble CD80 molecule could bind with CD28 to produce T cell costimulatory signal and also interact with CTLA-4, resulting in a CTLA-4-trap effect (Sugiura et al. 2019). Meanwhile, the interaction of soluble CD80 with PD-L1 can prevent PD-L1 from binding with PD-1 (Sugiura et al. 2019). Therefore, targeting CD80 emerges as a promising approach for advancing cancer immunotherapy.

Here, we initially expressed human and murine-derived CD80-Fc fusion proteins using 293F cells and determined their molecular weights by SDS-PAGE. Subsequently, we detected the affinity of CD80-Fc to the targets at the molecular level and found that CD80-Fc had a moderate affinity for the targets. CD80-Fc was also demonstrated to be effective in activating T lymphocytes and inhibiting tumor progression. In particular, we found that CD80-Fc fusion protein still exerted good anti-tumor activity even at a dosage of 0.25 mg/kg, which would greatly improve the safety of CD80-Fc administration. At the same time, the mice did not develop CRS-related symptoms at the doses we used. There also was no serious damage to major organs. This suggested that CD80-Fc did not induce a cytokine storm as severe as the CD28 agonistic antibody TGN1412. Moreover, we found that CD80-Fc fusion protein not only has a significant inhibitory effect on immunogenic tumors but also has an inhibitory effect on poor immunogenic tumors. However, the anti-tumor effect of CD80-Fc in cold tumors LLC was not as pronounced as in MC38 tumors which might be attributed to the relatively low infiltration of effector T cells in tumor tissues. The following in vivo lymphocyte migration blocking experiments demonstrated that the administration of FTY720 resulted in the effective blockade of T cell entry into the tumor, which completely reversed the anti-tumor activity of CD80-Fc. This indicates that effective T cell infiltration plays a pivotal role in the anti-tumor activity of CD80-Fc fusion protein; thus, improving immune infiltration through a combination strategy may further ensure the efficacy of CD80-Fc fusion protein.

It is noteworthy that during the treatment of LLC cold tumors, CD80-Fc did not significantly increase the infiltration of $CD4^+$ T cells in tumor tissues. $CD4^+$ T cells do not play a direct anti-tumor cytotoxic role like $CD8^+$ T cells but act as a helper T cell to regulate other immune cells and thus coordinate the immune response. There are several subtypes of $CD4^+$ T cells, such as Th1, Th2, Th17, and Treg cells. These subtypes have a variety of functions, some of which stimulate the immune response, and others,

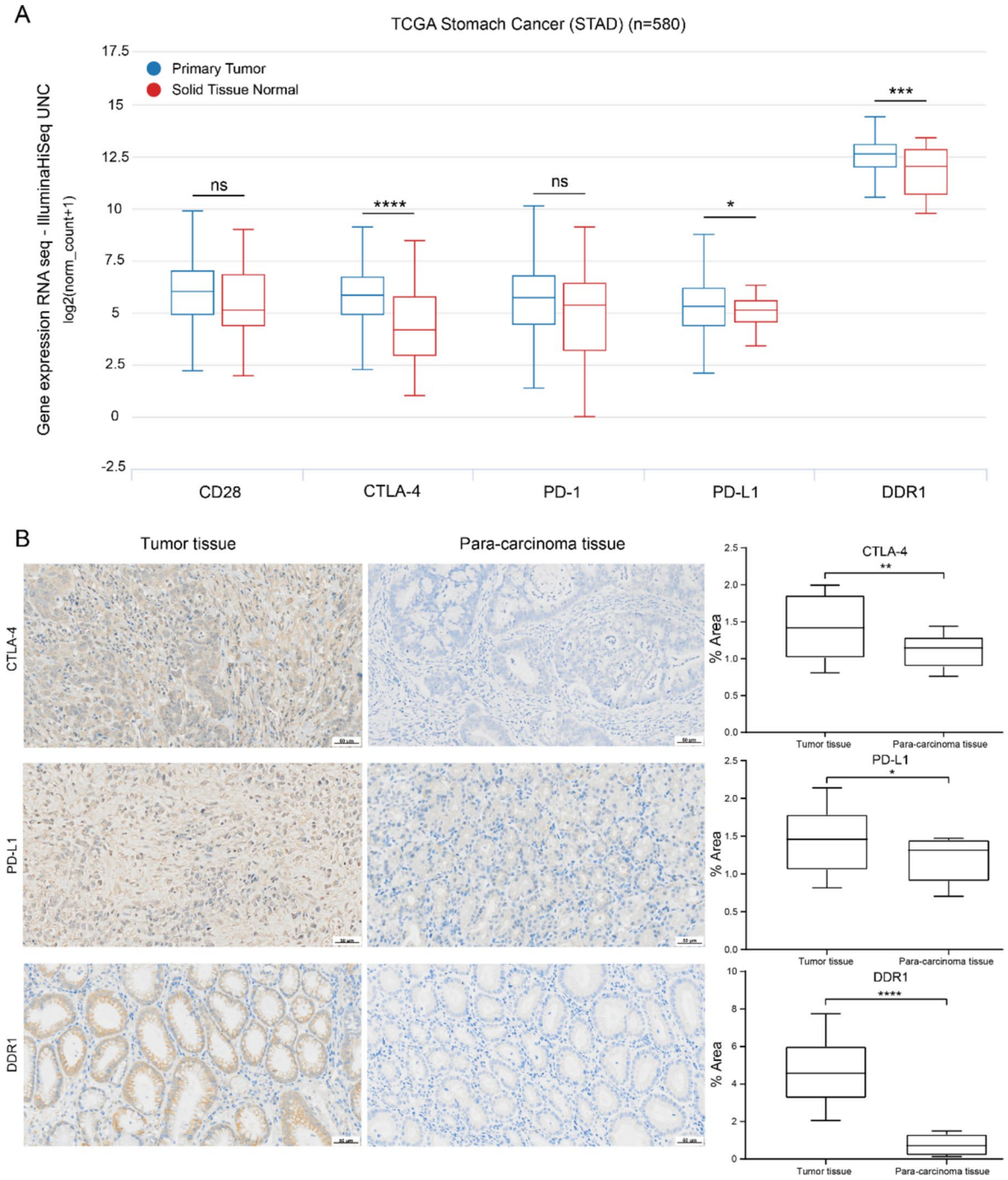

Fig. 6 Significant overexpression of CTLA-4, PD-L1, and DDR1 in the gastric cancer. **A** The mRNA expression levels of CD28, CTLA-4, PD-L1, PD-1, and DDR1 were examined in STAD using UCSC Xena database. The TCGA Stomach Cancer dataset includes 580 patient samples. Statistical analysis employed Welch's *t*-test for determining differences. **B** Immunohistochemical analysis of CTLA-4, PD-L1, and DDR1 in the clinical samples from 20 patients with gastric cancer. All pictures were photographed by VS200 full slide scanner. The cells that expressed CTLA-4, PD-L1, and DDR1 (brown staining) were counted with Image J software. Data were presented as mean ± SD

for example, Tregs, inhibit the immune response, which in turn affects the potential to detect CD4 as a direct indicator for anti-tumor cytotoxicity. Soluble CD80 molecules can interact with CTLA-4 on Tregs to produce a CTLA-4-trap effect. For example, GI-101 (a CD80 and IL2v fusion protein), which was developed by GI Innovation in collaboration with Simcere, could trap CTLA-4 (highly expressed on the surface of Tregs) then significantly decrease the

Tregs, especially in cold tumors (Wang et al. 2024). These alterations may ultimately result in no significant difference in the total number of $CD4^+$ T cells compared to the control group following treatment with CD80-Fc in LLC tumor. We think that the analysis of $CD4^+$ T cell subtypes can be made in further studies.

In our previous published work, a noteworthy association was uncovered between DDR1 and immune cell infiltration in gastric cancer (Wang et al. 2022). Furthermore, research indicated a downregulation of CD80 expression in gastric cancer in contrast to normal gastric mucosa, particularly noticeable in tissues of poorly differentiated gastric cancer (Feng et al. 2019). This decreased CD80 expression is strongly linked to reduced rates of both OS and DFS among patients with gastric cancer (Feng et al. 2019). So, CD80 is regarded as an independent prognostic factor for individuals diagnosed with gastric cancer. Therefore, we attempted to combine CD80-Fc fusion protein with a DDR1 inhibitor for the treatment of gastric cancer, which in turn further enhanced its anti-tumor effect. In a subsequent PBMCs-PDX gastric cancer model, hu-CD80-Fc fusion protein in combination with a DDR1 inhibitor demonstrated an enhanced capacity to foster T cell infiltration while significantly inhibiting tumor progression. Finally, we used bioinformatics and gastric cancer clinical samples to analyze the expression levels of PD-1, PD-L1, DDR1, CTLA-4, and CD28. The results showed that PD-L1, DDR1, and CTLA-4 were all highly expressed in gastric cancer. This also suggested that the combination of CD80-Fc fusion proteins with DDR1 inhibitors could offer a novel approach for clinical immunotherapy targeting gastric cancer. Of course, there are still shortcomings in our study, especially the experimental study on the mechanism of CD80 fusion protein combined with DDR1 inhibitor for the treatment of gastric cancer is not sufficient, which will be the focus of our next research.

Supplementary Information The online version contains supplementary material available at https://doi.org/10.1007/s00253-025-13419-z.

Acknowledgements The authors would like to thank the support of Beijing Beyond Biotechnology Co., Ltd in protein construction and expression.

Author contribution LY, SW, and PH conceived and designed the experiments. JZ and WH performed protein expression and purification. SW performed most of the experiments and data analyses. DP, XH, and HC contributed to data analysis. XZ, JF, DJ, and YZ provided technical support for experiment implementation. All authors contributed to the article and approved the submitted version.

Funding This study was supported by the Macau Science and Technology Development Fund (FDCT 0148/2022/A3 and 0019/2024/RIA1) and the Guangdong-Hong Kong-Macao University Joint Laboratory of Interventional Medicine Foundation of Guangdong Province (2023LSYS001).

Data availability All data generated or analyzed during this study are included in the article.

Declarations

Ethics approval The animal experiments were conducted according to guidelines evaluated and approved by the Institutional Animal Care and Use Committee (IACUC), School of Pharmacy, Fudan University (Shanghai, China). We declare that current research is in full compliance with ethical standards.

Consent for publication All authors listed on this manuscript have read and agreed to the publication of this research.

Conflict of interest The authors declare no competing interests.

References

Ambrogio C, Gómez-López G, Falcone M, Vidal A, Nadal E, Crosetto N, Blasco RB, Fernández-Marcos PJ, Sánchez-Céspedes M, Ren X, Wang Z, Ding K, Hidalgo M, Serrano M, Villanueva A, Santamaría D, Barbacid M (2016) Combined inhibition of DDR1 and Notch signaling is a therapeutic strategy for KRAS-driven lung adenocarcinoma. Nat Med 22(3):270–277. https://doi.org/10.1038/nm.4041

Azuma M (2019) Co-signal molecules in T-cell activation: historical overview and perspective. Adv Exp Med Biol 1189:3–23. https://doi.org/10.1007/978-981-32-9717-3_1

Bhatia S, Edidin M, Almo SC, Nathenson SG (2005) Different cell surface oligomeric states of B7–1 and B7–2: implications for signaling. Proc Natl Acad Sci U S A 102(43):15569–15574. https://doi.org/10.1073/pnas.0507257102

Boise LH, Minn AJ, Noel PJ, June CH, Accavitti MA, Lindsten T, Thompson CB (1995) CD28 costimulation can promote T cell survival by enhancing the expression of Bcl-XL. Immunity 3(1):87–98. https://doi.org/10.1016/1074-7613(95)90161-2

Chiba K (2005) FTY720, a new class of immunomodulator, inhibits lymphocyte egress from secondary lymphoid tissues and thymus by agonistic activity at sphingosine 1-phosphate receptors. Pharmacol Ther 108(3):308–319. https://doi.org/10.1016/j.pharmthera.2005.05.002

Das S, Johnson DB (2019) Immune-related adverse events and anti-tumor efficacy of immune checkpoint inhibitors. J Immunother Cancer 7(1):306. https://doi.org/10.1186/s40425-019-0805-8

Feng XY, Lu L, Wang KF, Zhu BY, Wen XZ, Peng RQ, Ding Y, Li DD, Li JJ, Li Y, Zhang XS (2019) Low expression of CD80 predicts for poor prognosis in patients with gastric adenocarcinoma. Future Oncol 15(5):473–483. https://doi.org/10.2217/fon-2018-0420

Gao Y, Zhou J, Li J (2021) Discoidin domain receptors orchestrate cancer progression: a focus on cancer therapies. Cancer Sci 112(3):962–969. https://doi.org/10.1111/cas.14789

Goldman MJ, Craft B, Hastie M, Repečka K, McDade F, Kamath A, Banerjee A, Luo Y, Rogers D, Brooks AN, Zhu J, Haussler D (2020) Visualizing and interpreting cancer genomics data via the Xena platform. Nat Biotechnol 38(6):675–678. https://doi.org/10.1038/s41587-020-0546-8

Hui E, Cheung J, Zhu J, Su X, Taylor MJ, Wallweber HA, Sasmal DK, Huang J, Kim JM, Mellman I, Vale RD (2017) T cell costimulatory receptor CD28 is a primary target for PD-1-mediated inhibition. Science 355(6332):1428–1433. https://doi.org/10.1126/science.aaf1292

Huynh J, Patel K, Gong J, Cho M, Malla M, Parikh A, Klempner S (2021) Immunotherapy in gastroesophageal cancers: current evidence and ongoing trials. Curr Treat Options Oncol 22(11):100. https://doi.org/10.1007/s11864-021-00893-6

Ikemizu S, Gilbert RJ, Fennelly JA, Collins AV, Harlos K, Jones EY, Stuart DI, Davis SJ (2000) Structure and dimerization of a soluble form of B7–1. Immunity 12(1):51–60. https://doi.org/10.1016/s1074-7613(00)80158-2

Intlekofer AM, Thompson CB (2013) At the bench: preclinical rationale for CTLA-4 and PD-1 blockade as cancer immunotherapy. J Leukoc Biol 94(1):25–39. https://doi.org/10.1189/jlb.1212621

Kamphorst AO, Wieland A, Nasti T, Yang S, Zhang R, Barber DL, Konieczny BT, Daugherty CZ, Koenig L, Yu K, Sica GL, Sharpe AH, Freeman GJ, Blazar BR, Turka LA, Owonikoko TK, Pillai RN, Ramalingam SS, Araki K, Ahmed R (2017) Rescue of exhausted CD8 T cells by PD-1-targeted therapies is CD28-dependent. Science 355(6332):1423–1427. https://doi.org/10.1126/science.aaf0683

Krummel MF, Allison JP (1996) CTLA-4 engagement inhibits IL-2 accumulation and cell cycle progression upon activation of resting T cells. J Exp Med 183(6):2533–2540. https://doi.org/10.1084/jem.183.6.2533

Larkin J, Chiarion-Sileni V, Gonzalez R, Grob JJ, Cowey CL, Lao CD, Schadendorf D, Dummer R, Smylie M, Rutkowski P, Ferrucci PF, Hill A, Wagstaff J, Carlino MS, Haanen JB, Maio M, Marquez-Rodas I, McArthur GA, Ascierto PA, Long GV, Callahan MK, Postow MA, Grossmann K, Sznol M, Dreno B, Bastholt L, Yang A, Rollin LM, Horak C, Hodi FS, Wolchok JD (2015) Combined nivolumab and ipilimumab or monotherapy in untreated melanoma. N Engl J Med 373(1):23–34. https://doi.org/10.1056/NEJMoa1504030

Lei Q, Wang D, Sun K, Wang L, Zhang Y (2020) Resistance mechanisms of anti-PD1/PDL1 therapy in solid tumors. Front Cell Dev Biol 8:672. https://doi.org/10.3389/fcell.2020.00672

Leitinger B (2014) Discoidin domain receptor functions in physiological and pathological conditions. Int Rev Cell Mol Biol 310:39–87. https://doi.org/10.1016/b978-0-12-800180-6.00002-5

Liu W, Zang X (2019) Structures of immune checkpoints: an overview on the CD28-B7 family. Adv Exp Med Biol 1172:63–78. https://doi.org/10.1007/978-981-13-9367-9_3

Nagai S, Azuma M (2019) The CD28-B7 family of co-signaling molecules. Adv Exp Med Biol 1189:25–51. https://doi.org/10.1007/978-981-32-9717-3_2

Parry RV, Chemnitz JM, Frauwirth KA, Lanfranco AR, Braunstein I, Kobayashi SV, Linsley PS, Thompson CB, Riley JL (2005) CTLA-4 and PD-1 receptors inhibit T-cell activation by distinct mechanisms. Mol Cell Biol 25(21):9543–9553. https://doi.org/10.1128/mcb.25.21.9543-9553.2005

Ribas A, Wolchok JD (2018) Cancer immunotherapy using checkpoint blockade. Science 359(6382):1350–1355. https://doi.org/10.1126/science.aar4060

Sansom DM (2000) CD28, CTLA-4 and their ligands: who does what and to whom? Immunology 101(2):169–177. https://doi.org/10.1046/j.1365-2567.2000.00121.x

Snanoudj R, Frangié C, Deroure B, François H, Créput C, Beaudreuil S, Dürrbach A, Charpentier B (2007) The blockade of T-cell co-stimulation as a therapeutic stratagem for immunosuppression: focus on belatacept. Biologics 1(3):203–213

Sugiura D, Maruhashi T, Okazaki IM, Shimizu K, Maeda TK, Takemoto T, Okazaki T (2019) Restriction of PD-1 function by cis-PD-L1/CD80 interactions is required for optimal T cell responses. Science 364(6440):558–566. https://doi.org/10.1126/science.aav7062

Sun X, Wu B, Chiang HC, Deng H, Zhang X, Xiong W, Liu J, Rozeboom AM, Harris BT, Blommaert E, Gomez A, Garcia RE, Zhou Y, Mitra P, Prevost M, Zhang D, Banik D, Isaacs C, Berry D, Lai C, Chaldekas K, Latham PS, Brantner CA, Popratiloff A, Jin VX, Zhang N, Hu Y, Pujana MA, Curiel TJ, An Z, Li R (2021) Tumour DDR1 promotes collagen fibre alignment to instigate immune exclusion. Nature 599(7886):673–678. https://doi.org/10.1038/s41586-021-04057-2

Suntharalingam G, Perry MR, Ward S, Brett SJ, Castello-Cortes A, Brunner MD, Panoskaltsis N (2006) Cytokine storm in a phase 1 trial of the anti-CD28 monoclonal antibody TGN1412. N Engl J Med 355(10):1018–1028. https://doi.org/10.1056/NEJMoa063842

Vackova J, Polakova I, Johari SD, Smahel M (2021) CD80 expression on tumor cells alters tumor microenvironment and efficacy of cancer immunotherapy by CTLA-4 blockade. Cancers (Basel) 13(8):1935. https://doi.org/10.3390/cancers13081935

Valiathan RR, Marco M, Leitinger B, Kleer CG, Fridman R (2012) Discoidin domain receptor tyrosine kinases: new players in cancer progression. Cancer Metastasis Rev 31(1–2):295–321. https://doi.org/10.1007/s10555-012-9346-z

Wang S, Fu Y, Kuerban K, Liu J, Huang X, Pan D, Chen H, Zhu Y, Ye L (2022) Discoidin domain receptor 1 is a potential target correlated with tumor invasion and immune infiltration in gastric cancer. Front Immunol 13:933165. https://doi.org/10.3389/fimmu.2022.933165

Wang S, Hu P, Fan J, Zou J, Hong W, Huang X, Pan D, Chen H, Zhu YZ, Ye L (2024) CD80-Fc fusion protein as a potential cancer immunotherapy strategy. Antib Ther 7(1):28–36. https://doi.org/10.1093/abt/tbad029

Xu F, Jin T, Zhu Y, Dai C (2018) Immune checkpoint therapy in liver cancer. J Exp Clin Cancer Res 37(1):110. https://doi.org/10.1186/s13046-018-0777-4

Yokosuka T, Takamatsu M, Kobayashi-Imanishi W, Hashimoto-Tane A, Azuma M, Saito T (2012) Programmed cell death 1 forms negative costimulatory microclusters that directly inhibit T cell receptor signaling by recruiting phosphatase SHP2. J Exp Med 209(6):1201–1217. https://doi.org/10.1084/jem.20112741